B.A.N. **17,** no 2, 115–126; *Communication from the Kapteyn Astronomical Laboratory, Groningen*

THE LAW OF INTERSTELLAR EXTINCTION

H. L. JOHNSON

Lunar and Planetary Laboratory, University of Arizona, Tucson, Arizona

and

J. BORGMAN

Kapteyn Astronomical Laboratory, Groningen

Received December 20, 1962

Photoelectric and photoconductive photometry of early-type stars in 5, 7 or 8 wavelength regions is given. The observations extend from 3500 Å in the ultraviolet to 3.5 μ in the infrared. The analysis is based on the colour excesses derived from the intrinsic colours. It is shown that there is no unique reddening law; neither is the ratio of visual to selective extinction constant. Probably the situation can be best described by a minor continuous variation of this ratio with galactic longitude, with some deviations to larger values in regions of hot stars. The largest deviation seems to be in the Orion Nebula region, where a value of $A_V/E_{B-V} = 7.4$ has been found.

1. Introduction

Recently the authors (BORGMAN and JOHNSON, 1962) have reported briefly on measurements of the interstellar reddening law. The observations extended to about 8400 Å in the infrared. Since then more stars have been observed, several of them to 2.2 μ and, for a few selected stars, data are now available at 3.5 μ. The new observations make possible the study of interstellar extinction over a wide wavelength range and we will show that this results in a rather direct and accurate estimate of the ratio of visual to selective extinction. The latter quantity is usually derived from statistical studies in star clusters and almost invariably a value close to 3 has been found (WHITFORD, 1958). The only serious deviation from this value seems to be SHARPLESS' (1952) estimate of 6 for the Orion region. Precise knowledge of the ratio of visual to selective extinction is of importance for the determination of photometric distances of reddened stars or clusters.

2. Instruments and observations

All observations have been obtained with the 82-inch and 36-inch telescopes of the McDonald Observatory. 5, 7 or 8 filters have been used, depending on the infrared brightness of the star. The designations of the filters are: U, B, V, R, I, J, K and L. Some of these filter designations are the same as have been used by BORGMAN (1961) in an investigation of the reddening law. However, the two filter sets have no type in common and the similarity of designations is incidental. The *U*, *B* and *V* measurement are on the *UBV* system (JOHNSON, 1951). *R*, *I*, *J*, *K* and *L* refer to red and infrared observations. A description of the photometric apparatus, including the measured response curves of the filter bands, is given by JOHNSON and MITCHELL (1962). The red and infrared systems (*RIJKL*) are to be considered tentative in the sense that small zero-point corrections may be made in the future. Such corrections have no consequences for the conclusions presented in this paper.

TABLE 1

Characteristics of filters

Filter	λ_m	λ_e	λ_m^{-1}	λ_e^{-1}
U	3540 Å	3450 Å	2.82 μ^{-1}	2.90 μ^{-1}
B	4430	4340	2.26	2.30
V	5550	5470	1.80	1.83
R	6720	6420	1.49	1.56
I	8700	8400	1.15	1.19
J	1.20 μ	1.16 μ	0.83	0.86
K	2.20	2.14	0.45	0.47
L	3.50	3.37	0.29	0.30

TABLE 2

Photometric observations

	HD	Name or BD	l^{II}	b^{II}	MK	V	$U-V$	$B-V$	$V-R$	$V-I$	$V-J$	$V-K$	$V-L$
			°	°		m	m	m	m	m	m	m	
	2905	κ Cas	120.8	+ 0.1	B1Ia	4.17	− 0.65	+ 0.14	+ 0.04	+ 0.16	+ 0.18	+ 0.21	
	10516	φ Per	131.3	− 11.3	B2pe	4.07	− 0.96	− 0.03	+ 0.06	+ 0.12	+ 0.26	+ 0.71	
	12993		133.1	− 3.4	O5	8.97	− 0.61	+ 0.18	+ 0.12	+ 0.26			
	14434		135.1	− 3.8	O6	8.51	− 0.62	+ 0.17	+ 0.10	+ 0.23			
	14633		140.8	− 18.2	O8V	7.45	− 1.29	− 0.21	− 0.15	− 0.31			
	15558		134.7	+ 0.9	O6	7.88	− 0.04	+ 0.51	+ 0.42	+ 0.88			
	15570		134.8	+ 0.8	O5f	8.11	+ 0.30	+ 0.69	+ 0.59	+ 1.20	+ 1.52	+ 1.66	
	15629		134.8	+ 1.0	O5	8.41	− 0.19	+ 0.43	+ 0.34	+ 0.73			
	17088		137.9	− 1.8	B9Ia	7.54	+ 0.87	+ 0.78	+ 0.58	+ 1.30			
	17145		138.0	− 1.8	B8Ia	8.07	+ 0.86	+ 0.83	+ 0.61	+ 1.31			
	17520		137.2	+ 0.9	O8V	8.26	− 0.36	+ 0.31	+ 0.21	+ 0.47			
*	21291		141.5	+ 2.9	B9Ia	4.21	+ 0.18	+ 0.41	+ 0.28	+ 0.71	+ 1.03	+ 1.22	
*	21389		142.2	+ 2.1	A0Ia	4.55	+ 0.46	+ 0.56	+ 0.42	+ 0.96	+ 1.33	+ 1.65	
*	24398	ζ Per	162.3	− 16.7	B1Ib	2.87	− 0.67	+ 0.09	+ 0.05	+ 0.17	+ 0.23	+ 0.21	
*	24912	ξ Per	160.4	− 13.1	O7	4.05	− 0.92	0.00	+ 0.04	+ 0.07	+ 0.11	+ 0.01	
	34085	β Ori	209.2	− 25.3	B8Ia	0.10	− 0.72	− 0.03	− 0.08	− 0.08	− 0.11	− 0.10	− 0.17
	36512	υ Ori	210.4	− 21.0	B0V	4.63	− 1.33	− 0.26	− 0.14	− 0.36			
	36591		205.1	− 18.2	B1V	5.35	− 1.08	− 0.16	− 0.14	− 0.28			
	36629		207.9	− 19.5	B2V	7.66	− 0.63	+ 0.02	+ 0.10	+ 0.15			
	37020	θ^1A Ori	209.0	− 19.4	B0,5Vp	6.72	− 0.87	0.00	+ 0.24	+ 0.49			
	37022	θ^1C Ori	209.0	− 19.4	O6p	5.13	− 0.95	− 0.01	+ 0.14	+ 0.36			
	37023	θ^1D Ori	209.0	− 19.4	B0,5Vp	6.70	− 0.75	+ 0.08	+ 0.22	+ 0.46			
**		θ^1 Ori	209.0	− 19.4		4.60	− 0.88	+ 0.02	+ 0.16	+ 0.45	+ 0.58	+ 1.02	
	37041	θ^2 Ori	209.1	− 19.4	O9,5Vp	5.06	− 1.02	− 0.08	+ 0.06	+ 0.10	+ 0.20	+ 0.34	
	37042		209.1	− 19.4	B1V	6.40	− 1.01	− 0.09	+ 0.06	+ 0.08			
*	37043	ι Ori	209.1	− 19.6	O9III	2.76	− 1.30	− 0.24	− 0.15	− 0.30	− 0.51	− 0.77	
	37061		208.9	− 19.3	B1V	6.85	− 0.36	+ 0.27	+ 0.38	+ 0.78			
	37903		206.9	− 16.5	B1,5V	7.82	− 0.49	+ 0.11	+ 0.16	+ 0.34			
*	38771	κ Ori	214.5	− 18.5	B0,5Ia	2.07	− 1.18	− 0.18	− 0.07	− 0.20	− 0.51	− 0.58	
**	38899	134 Tau	194.5	− 7.6	B9IV	4.89	− 0.21	− 0.05	− 0.06	− 0.10			
*	41117	χ^2 Ori	189.7	− 0.9	B2Ia	4.62	− 0.41	+ 0.28	+ 0.20	+ 0.46	+ 0.51	+ 0.75	
	46106		206.2	− 2.1	B0,5V	7.92	− 0.61	+ 0.13	+ 0.08	+ 0.21			
	46149		206.2	− 2.0	O8	7.63	− 0.62	+ 0.17	+ 0.15	+ 0.30			
	46150	12 Mon	206.3	− 2.1	O6	6.78	− 0.71	+ 0.13	+ 0.17	+ 0.30	+ 0.40	+ 0.58	
	46202		206.3	− 2.0	O9V	8.18	− 0.57	+ 0.18	+ 0.14	+ 0.31			
	46223		206.5	− 2.1	O5	7.30	− 0.56	+ 0.22	+ 0.24	+ 0.44	+ 0.50	+ 0.82	
	46573		208.7	− 2.7	O7	7.92	− 0.29	+ 0.34	+ 0.24	+ 0.54			
	47839	15 Mon	202.9	+ 2.2	O7	4.65	− 1.30	− 0.22	− 0.18	− 0.36			
	48099		206.2	+ 0.8	O6	6.38	− 0.97	− 0.04	− 0.01	− 0.02			
	66811	ζ Pup	256.0	− 4.7	O5f	2.25	− 1.37	− 0.26	− 0.17	− 0.37	− 0.54	− 0.77	
**	91316	ρ Leo	234.9	+ 52.8	B1Ib	3.85	− 1.08	− 0.12	− 0.11	− 0.19	− 0.34	− 0.46	
	149757	ζ Oph	6.3	+ 23.6	O9,5V	2.58	− 0.83	+ 0.02	+ 0.09	+ 0.04	− 0.05	− 0.08	
	163800		7.1	+ 0.7	O8	7.01	− 0.38	+ 0.29	+ 0.35	+ 0.55	+ 0.64	+ 0.61	
	166734		18.9	+ 3.6	O8f	8.43	+ 0.94	+ 1.08	+ 1 00	+ 1.90	+ 2.51	+ 3.04	
	167330		17.7	+ 2.2	O9I-II	8.23	+ 0.21	+ 0.66	+ 0.63	+ 1.19			
	167971		18.2	+ 1.7	O8f	7.52	+ 0.43	+ 0.76	+ 0.77	+ 1.40	+ 1.88	+ 2.28	
**	168112		18.4	+ 1.6	O6	8.52	+ 0.26	+ 0.67	+ 0.66	+ 1.22			
	183143		53.2	+ 0.6	B7Ia	6.87	+ 1.36	+ 1.20	+ 1.08	+ 2.03	+ 2.79	+ 3.41	+3.85
	184279		41.1	− 7.6	B0,5IV	6.89	− 0.77	+ 0.03	+ 0.13	+ 0.15			
	184915		31.8	− 13.3	B0,5III	4.98	− 0.87	0.00	+ 0.04	+ 0.03			

TABLE 2 *(continued)*

HD	Name or BD	l^{II}	b^{II}	MK	V	$U-V$	$B-V$	$V-R$	$V-I$	$V-J$	$V-K$	$V-L$
		°	°		m	m	m	m	m	m	m	m
188209		81.0	+ 10.1	O9,5III	5.63	− 1.07	− 0.10	+ 0.01	− 0.07			
190864		72.5	+ 2.0	O6	7.76	− 0.60	+ 0.18	+ 0.23	+ 0.39			
193237	P Cyg	75.8	+ 1.3	P Cyg	4.81	− 0.16	+ 0.42	+ 0.45	+ 0.74	+ 1.07	+ 1.55	
193322		78.1	+ 2.8	O8	5.83	− 0.67	+ 0.11	+ 0.08	+ 0.14			
193514		77.0	+ 1.8	O7f	7.40	− 0.09	+ 0.43	+ 0.41	+ 0.79			
193595		76.9	+ 1.6	O7	8.73	− 0.23	+ 0.36	+ 0.31	+ 0.62			
193682		75.9	+ 0.8	O5	8.40	+ 0.03	+ 0.50	+ 0.43	+ 0.81			
** 195213		79.3	+ 1.2	O7	8.73	+ 0.58	+ 0.83	+ 0.77	+ 1.50			
* 195592		82.4	+ 3.0	O9,5Ia	7.08	+ 0.66	+ 0.88	+ 0.70	+ 1.43	+ 1.98	+ 2.44	
197345	α Cyg	84.3	+ 2.0	A2Ia	1.26	− 0.16	+ 0.09	+ 0.12	+ 0.15	+ 0.23	+ 0.35	+ 0.43
** 198478	55 Cyg	85.8	+ 1.5	B3Ia	4.81	− 0.06	+ 0.40	+ 0.27	+ 0.62			
** 204710		89.7	− 4.5	B8Ib	6.94	+ 0.02	+ 0.26	+ 0.20	+ 0.52			
207198		103.1	+ 7.0	O9II	5.91	− 0.31	+ 0.32	+ 0.18	+ 0.41	+ 0.50	+ 0.56	
* 207260		102.3	+ 5.9	A2Ia	4.28	+ 0.66	+ 0.53	+ 0.40	+ 0.88	+ 1.12	+ 1.46	
210839	λ Cep	103.8	+ 2.6	O6f	5.05	− 0.49	+ 0.24	+ 0.19	+ 0.37	+ 0.43	+ 0.47	
214680	10 Lac	96.7	− 17.0	O9V	4.87	− 1.24	− 0.20	− 0.17	− 0.33	− 0.55	− 0.77	
	+ 56° 739	139.0	− 1.6	O9,5Ib	9.92	+ 0.93	+ 1.00	+ 0.77	+ 1.54			
	+ 61° 411	133.8	+ 1.2	O8:	10.08	+ 0.88	+ 0.98	+ 0.78	+ 1.57			
	+ 60° 497	134.6	+ 0.9	O7	8.78	+ 0.02	+ 0.57	+ 0.46	+ 0.95			
	+ 28° 4211	81.8	− 19.3	Op	10.49	− 1.57	− 0.32	− 0.23	− 0.51			
	− 12° 4964	18.1	+ 1.8	O8	9.81	+ 0.67	+ 0.90	+ 0.84	+ 1.59			
	− 12° 5009	18.6	+ 1.2	O8	9.54	+ 0.23	+ 0.64	+ 0.64	+ 1.18			
164794	NGC6530 7	6.0	− 1.2	O5	5.98	− 0.95	+ 0.02	+ 0.16	+ 0.22	+ 0.22	+ 0.13	
** 164816	NGC6530 9	6.1	− 1.2	B0V	7.09	− 0.90	− 0.02	+ 0.13	+ 0.13			
** 165052	NGC6530 118	6.1	− 1.5	O7	6.86	− 0.77	+ 0.07	+ 0.22	+ 0.34			
	NGC6611 1			(O)	8.25	− 0.12	+ 0.47	+ 0.54	+ 0.98	+ 1.22	+ 1.50	
	NGC6611 4			(O)	8.96	− 0.20	+ 0.42	+ 0.45	+ 0.85			
	NGC6611 5			O9.5V	9.46	− 0.42	+ 0.27	+ 0.31	+ 0.50			
	NGC6611 7	17.0	+ 0.8	O5	9.59	+ 0.66	+ 0.90	+ 0.92	+ 1.72			
	NGC6611 9			(O)	9.88	− 0.18	+ 0.62	+ 0.66	+ 1.21			
	NGC6611 197			(O)	8.78	− 0.10	+ 0.47	+ 0.49	+ 0.90			
**	NGC6823 2	59.4	− 0.1	O7	9.34	0.00	+ 0.56	+ 0.46	+ 0.95			
**	NGC6823 4			B0IV	9.74	− 0.17	+ 0.41	+ 0.31	+ 0.66			
229196	NGC6910 3	78.8	+ 2.1	O5	8.52	+ 0.71	+ 0.90	+ 0.78	+ 1.54	+ 2.07	+ 2.45	
	VI Cyg 6			O8(V)	10.65	+ 1.35	+ 1.21	+ 1.02	+ 1.95			
	VI Cyg 7			O6f	10.47	+ 1.69	+ 1.42	+ 1.27	+ 2.36			
**	VI Cyg 8A	80.2	+ 0.8	O6f	9.03	+ 1.39	+ 1.24	+ 1.12	+ 2.07			
*	VI Cyg 9			O5f	10.78	+ 2.64	+ 1.90	+ 1.73	+ 3.03	+ 4.18	+ 5.17	
*	VI Cyg 10			O9Ia	9.86	+ 1.89	+ 1.50	+ 1.36	+ 2.56	+ 3.42	+ 4.22	
	VI Cyg 12			B8Ia	11.49	+ 5.72	+ 3.22	+ 3.13	+ 5.29	+ 6.94	+ 8.68	+ 9.17

* J and K observed only once.
** U, B, V, R and I observed only once.

Some characteristics of the filters are given in table 1. λ_m is a quantity defined by

$$\lambda_m = \frac{\int \lambda S(\lambda)\, d\lambda}{\int S(\lambda)\, d\lambda}.$$

$S(\lambda)$ is the relative response of the filter-cell combination. λ_e is defined by

$$\lambda_e = \frac{\int \lambda S(\lambda) I(\lambda)\, d\lambda}{\int S(\lambda) I(\lambda)\, d\lambda},$$

$I(\lambda)$ being the intensity distribution of a black body at 22 000 °K. The wavelength λ_e corresponds more closely to the wavelength for which the observed extinctions are valid. The problems in connection with the effective wavelength of the wide band filters used in the present investigation will be discussed further in section 5 of this paper.

Table 2 lists the observations in the form of 7 colour indices ($U-V$, $B-V$, $V-R$, $V-I$, $V-J$, $V-K$ and $V-L$) and the visual magnitude V. The MK classifications have been taken from various sources in the literature (JOHNSON and MORGAN, 1953, 1955; HILTNER and JOHNSON, 1956; HILTNER, 1956; JOHNSON *et al.*, 1961). A few O stars in NGC 6611 have their spectral type in parentheses. This means that the classification has been assigned on the basis of the so-called Q-method as it has been modified and described by JOHNSON (1958). The accuracy of these spectral types is low but adequate for the present purpose. Except when noted each star has been observed at least twice. The probable errors of one observation are approximately: U, $0^m.02$; B, $0^m.015$; V, $0^m.013$; R, I, J and K, $0^m.02$; L, $0^m.03$.

The galactic longitude l^{II} and latitude b^{II} are on the new system (BLAAUW *et al.*, 1960).

3. Intrinsic colours

Our study of the reddening law will be based on colour excesses of the stars in table 2. In this section we will describe the procedure of obtaining the intrinsic colours which have been given in table 3.

The data in table 2 include 5 blue O stars (ι Ori, ζ Pup, 10 Lac, HD 14633 and HD 47839) of average spectral type O8, corresponding to an intrinsic colour $(B-V)_0 = 0^m.31$ (JOHNSON, 1958). Using the ratio $E_{U-V}/E_{B-V} = 1.72$ we find the average intrinsic $U-V$ value to be: $(U-V)_0 = -1^m.46$; this is in good agreement with JOHNSON's (1958) value $-1^m.44$. Probably the value of E_{U-V}/E_{B-V} is not constant (WAMPLER, 1961) but the variation is small and for minor reddening corrections unimportant. The other intrinsic colours of O stars in table 3 have been derived from figures 1 and 2. These diagrams give plots of $V-R$, $V-I$, $V-J$ and $V-K$ against $B-V$. Each of the diagrams shows the property of increasing scatter with reddening which must be due to variations of the reddening law. The same characteristic (but less pronounced) has been found and analyzed earlier in a diagram based on colour indices in the visible region of the spectrum (BORGMAN, 1961, figure 3). We have plotted in figures 1 and 2 only stars with little reddening in order to avoid complications due to possible curvature of the reddening lines. In each diagram we have drawn the estimated trajectories of the two reddening lines with maximum and minimum slopes, taking into account that they must intersect at $B-V = -0^m.31$.

TABLE 3
Intrinsic colours

MK	Source	$(U-V)_0$	$(B-V)_0$	$(V-R)_0$	$(V-I)_0$	$(V-J)_0$	$(V-K)_0$	$(V-L)_0$
		m	m	m	m	m	m	m
O	Fig. 1 and 2	− 1.46	− 0.31	− 0.24	− 0.51	− 0.70	− 1.06	
B0V	υ Ori	− 1.40	− 0.30	− 0.18	− 0.45			
B0.5V	Interpolated	− 1.30	− 0.28	− 0.17	− 0.43			
B1V	Interpolated	− 1.20	− 0.26	− 0.17	− 0.41			
B1.5V	Interpolated	− 1.16	− 0.25	− 0.16	− 0.39			
B2V	Interpolated	− 1.11	− 0.24	− 0.15	− 0.38			
B9IV	134 Tau	− 0.23	− 0.06	− 0.07	− 0.12			
B0.51a	κ Ori	− 1.21	− 0.20	− 0.09	− 0.25	− 0.57	− 0.67	
B1IB	ρ Leo	− 1.18	− 0.18	− 0.17	− 0.29	− 0.52	− 0.73	
B1Ia	Interpolated	− 1.20	− 0.19	− 0.13	− 0.27	− 0.54	− 0.70	
B2Ia	Interpolated	− 1.12	− 0.17	− 0.12	− 0.24	− 0.48	− 0.63	
B3Ia	Interpolated	− 1.02	− 0.13	− 0.11	− 0.20	− 0.39	− 0.49	
B7Ia	Interpolated	− 0.80	− 0.04	− 0.08	− 0.10	− 0.14	− 0.15	− 0.24
B8Ia	β Ori	− 0.72	− 0.03	− 0.08	− 0.08	− 0.11	− 0.10	− 0.17
B9Ia	Interpolated	− 0.62	− 0.02	− 0.05	− 0.06	− 0.08	− 0.05	− 0.08
A0Ia	Interpolated	− 0.52	− 0.02	− 0.02	− 0.04	− 0.04	0.00	0.00
A2Ia	α Cyg	− 0.33	0.00	+ 0.04	0.00	+ 0.03	+ 0.10	+ 0.17

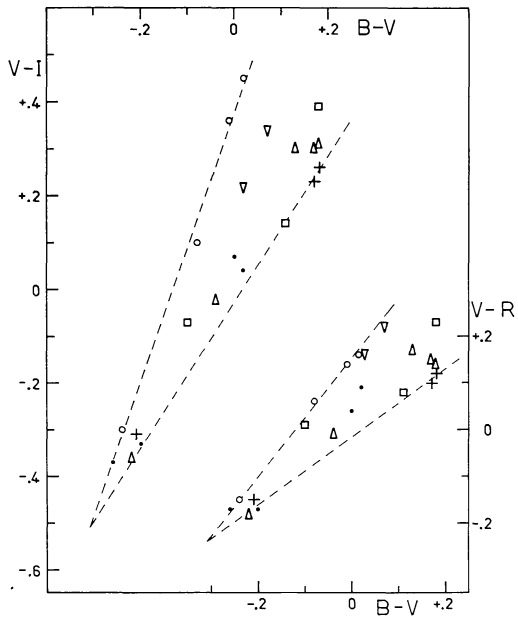

Fig. 1. $V - I$ and $V - R$ versus $B - V$ for the O stars in table 2 with $B - V \leqslant +0^{m}.20$.
open circles: Orion;
crosses: Perseus double cluster region;
triangles: Monoceros;
inverted triangles: NGC 6530;
squares: Cygnus;
dots: other regions.

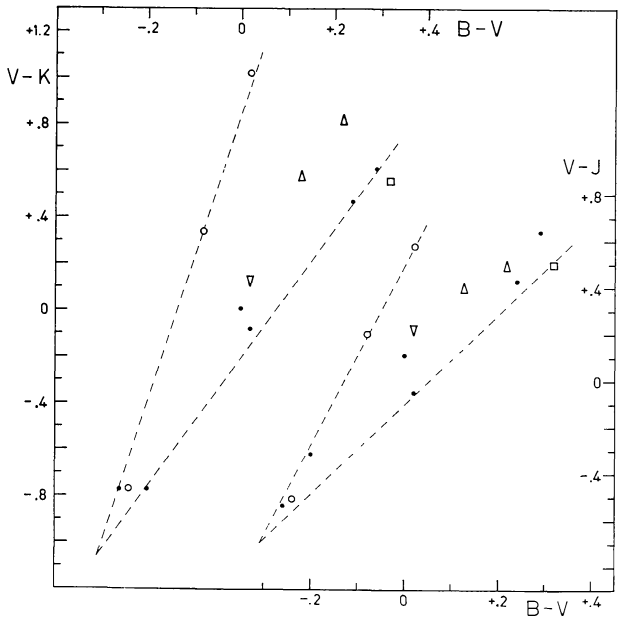

Fig. 2. $V - K$ and $V - J$ versus $B - V$ for the O stars in table 2 with $B - V \leqslant 0^{m}.40$. The symbols have the same meaning as in figure 1.

The intrinsic colours $(V - R)_0$, $(V - I)_0$, $(V - J)_0$ and $(V - K)_0$ are the corresponding ordinates in the diagrams; the numerical values have been entered into table 3 as intrinsic colours of an average O star.

The intrinsic colours of spectral type B0V have been derived from the well observed standard star υ Ori. This star shows a colour excess $E_{B-V} = +0^{m}.04$ over the intrinsic colour $(B - V)_0 = -0^{m}.30$ (JOHNSON, 1958). The other intrinsic colours of this star have been computed using the following colour-excess ratios: $E_{U-V}/E_{B-V} = 1.72$; $E_{V-R}/E_{B-V} = 1.01$; $E_{V-I}/E_{B-V} = 2.26$. The latter two are mean values of the extreme reddening line slopes in figure 1. The intrinsic colours of B0.5V, B1V, B1.5V and B2V have been interpolated between B0V and B9IV; for the intrinsic colours of B9IV we have adopted those of 134 Tau, after slight corrections for reddening, computed in the same way as has been pointed out for υ Ori. The interpolation is linear on the basis of the $(B - V)_0$ colours, which have been taken from JOHNSON (1958).

The small reddening corrections in the case of κ Ori and ρ Leo have been computed in accordance with the procedure used for υ Ori. There are two more colours to be derived: $(V - J)_0$ and $(V - K)_0$ were computed using the colour-excess ratios $E_{V-J}/E_{B-V} = 3.0$ and $E_{V-K}/E_{B-V} = 4.5$. These values are mean values of the extreme slopes in figure 2. Since the corrections for reddening are small it is not important that the actual colour-excess ratios between these extremes are unknown at this stage of the reduction. The adopted intrinsic colours of B1Ia are the mean of B0.5Ia and B1Ib. β Ori has been assumed unreddened; the observed colours have been entered into table 3 as intrinsic colours for B8Ia. The intrinsic colours of A2Ia are based on α Cyg. According to JOHNSON (1958) the intrinsic $B - V$ colour is $0^{m}.00$, which corresponds to a colour excess of $+0^{m}.09$. Though this colour excess is still small a realistic estimate of the colour-excess ratios instead of an average value could return more accurate intrinsic colours. Many data on the Cygnus region are available and will be discussed later in this paper. We have adopted for the present purpose the following colour-excess ratios: $E_{U-V}/E_{B-V} = 1.9$; $E_{V-R}/E_{B-V} = 0.8$; $E_{V-I}/E_{B-V} = 1.7$; $E_{V-J}/E_{B-V} = 2.2$; $E_{V-K}/E_{B-V} = 2.8$; $E_{V-L}/E_{B-V} = 2.9$. The resulting intrinsic colours have been entered in table 3 for A2Ia.

The intrinsic colours of the spectral types B2Ia, B3Ia, B7Ia, B9Ia and A0Ia have been interpolated between B1Ia, B8Ia and A2Ia. For the interpolation we have again been guided by the intrinsic $B - V$ colours as have been given by JOHNSON (1958). $(V - L)_0$ for B7Ia has been extrapolated from B8Ia and A2Ia.

4. Colour-excess ratios

The intrinsic colours of table 3 enable us to derive colour excesses for the stars in table 2. The colour excesses will be used for the computation of colour-excess ratios, all with E_{B-V} in the denominator.

The most interesting colour-excess ratio of the present material is E_{V-L}/E_{B-V}, the numerical value of which is expected to be only slightly less than $A_V/E_{B-V} = R$, the ratio of visual to selective extinction on the BV system. There are only two sufficiently reddened stars in table 2 with observed $V - L$ colours: HD 183143 and VI Cygni No. 12. The colour excesses on the $V - L$ scale are $4^m.09$ and $9^m.44$, resp., while the $B - V$ colour excesses are $1^m.24$ and $3^m.25$, resp. The resulting colour-excess ratios E_{V-L}/E_{B-V} are 3.30 and 2.90, resp., with a weighted mean value of 3.01 (weight $= E_{B-V}$). This is close to the usually adopted value of 3.0 to 3.2 for A_V/E_{B-V}. The interstellar extinction at the wavelength region transmitted by the L filter (approximately 3.4 μ) must be very small, probably less than 6% (corresponding to $A_V/E_{B-V} = = 3.2$) of the visual extinction, which is in agreement with VAN DE HULST'S (1949) theoretical extinction curves. Our computation of E_{V-L}/E_{B-V} for VI Cygni No. 12 is based on the classification B8Ia which follows from unpublished multicolour photometry by Borgman. If we adopt the classification B5Ia as given by SHARPLESS (1957) the colour-excess ratio changes only slightly (2.92 instead of 2.90). The extremely large reddening of this star makes knowledge of accurate intrinsic colours relatively unimportant.

Unfortunately the $V - L$ data are scarce but many stars in table 2 have $V - K$ observations. The two stars discussed above (HD 183143 and VI Cygni No. 12) show colour-excess ratios E_{V-K}/E_{B-V} of 2.87 and 2.70, resp.; the weighted mean value 2.75 is only 9% less than E_{V-L}/E_{B-V} and only 8–14% less than A_V/E_{B-V} (the range corresponds to the range 3.0–3.2 for A_V/E_{B-V}, quoted above). In the next section we will show that the interstellar extinction at the wavelength region of the K filter is 9% of the visual extinction; this conclusion pertains to the Cygnus stars of table 4a.

Apparently E_{V-K}/E_{B-V} is only slightly less than A_V/E_{B-V}; therefore, it is of particular interest to investigate variations of E_{V-K}/E_{B-V}. In figure 3 we have

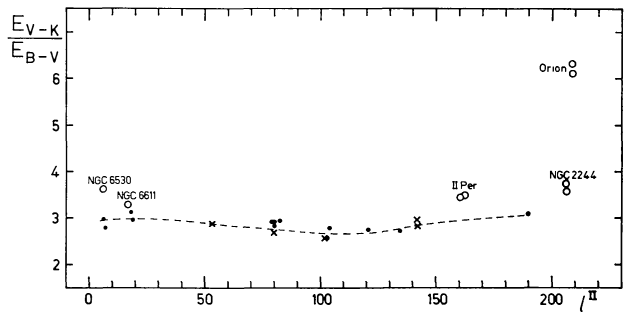

Fig. 3. E_{V-K}/E_{B-V} versus galactic longitude for all stars in table 2 with $E_{B-V} \geqslant 0^m.20$.
Open circles refer to stars in the indicated cluster or association, crosses are late B-type supergiants.
The dotted line is the estimated smooth variation when the open circles are omitted.

plotted this colour-excess ratio against galactic longitude l^{II} for stars in table 2 with $E_{B-V} \geqslant 0^m.20$. A few large colour-excess ratios have been marked, the largest of which are the two stars in the Orion Nebula (θ^2 Ori and the Trapezium θ^1 Ori). The deviation of the Orion stars is at least in qualitative agreement with Sharpless' statement that A_V/E_{B-V} in the Orion region must be close to 6. In the next section we will interpret variations of E_{V-K}/E_{B-V} as an indication of variations of A_V/E_{B-V}. It may be in order to discuss now the following alternative explanations of the variation of E_{V-K}/E_{B-V}, which deal especially with the most extreme case of the stars in the Orion Nebula region.

1. The assigned intrinsic colours of the Orion stars could be incorrect due to a peculiar energy distribution. Our computation of E_{V-K}/E_{B-V} is based on the intrinsic colours of an average O star, as given in table 3. However, θ^2 Ori has been classified as a peculiar O star, while θ^1 Ori is composed of one O6p star and 3 fainter early B stars, resulting in a composite spectrum with intrinsic colours of a late O star. If we wish to accept the explanation of anomalous intrinsic colours we must account for the fact that both θ^1 Ori and θ^2 Ori show the peculiar energy distribution in the same sense,

while the degree of anomaly is about proportional to the reddening. This statement follows from an inspection of figure 2: θ^2 Ori is reddened by about $\frac{2}{3}$ of the amount of θ^1 Ori, while both are in the $V-K$, $B-V$ diagram of figure 2 on the steepest reddening line which goes through the point corresponding to the adopted intrinsic colours. The explanation by an anomalous energy distribution appears to be unlikely.

2. The assigned intrinsic colours could be incorrect due to unrecognized red companions. Indeed, it is not difficult to construct combinations of the four trapezium stars with one or more later type stars that produce the large deviation of E_{V-K}/E_{B-V} in figure 3. E.g. α Tau (K5III) has about the right luminosity and colours: $M_V = -1^m.0$, $M_B = +0^m.5$ and $M_K = -4^m.6$; these absolute magnitudes follow from published photometry (JOHNSON and MORGAN, 1953; JOHNSON, 1962) and the trigonometric parallax. It is obvious that a companion with these characteristics should have negligible influence on the visual brightness and the $B-V$ colour of θ^1 Ori, for which we adopt $M_V = -5^m.9$, $M_B = -6^m.2$ and $M_K = -4^m.9$; however, the colour $V-K$ of the combination should be considerably redder. In the $V-K$, $B-V$ diagram of figure 2 the deviation of θ^1 Ori from the reddening line with smallest slope is about 1 magnitude in the $V-K$ direction. Such a deviation can be obtained by combining the four early-type trapezium stars with 3 companions of the characteristics of α Tau. We are confident that it will be possible to construct a combination of stars that explains at the same time the deviation in the $V-J$, $B-V$ diagram of figure 2 and the much smaller deviations in the diagrams of figure 1. However, we must also account for the similar but less pronounced behaviour of θ^2 Ori. It is clear that we can repeat here our objections pointed out in connection with the previous hypothesis of a peculiar energy distribution of the four Trapezium stars.

We prefer to accept the simpler explanation of a variable reddening law. This conclusion is also in agreement with the general picture of figures 1 and 2: the scatter increases with reddening. It would be hard to account for this fact by adopting one of the two alternative explanations discussed above. In addition we can make a rough independent check on the large value of E_{V-K}/E_{B-V}, which should be close to A_V/E_{B-V}. The latter ratio can be estimated independently from the spectroscopic and photometric data of θ^1 Ori. The trapezium, consisting of one O star and 3 early B stars should have an absolute visual brightness of $-5^m.9$ (JOHNSON and IRIARTE, 1958). Combined with a distance modulus of $8^m.1$ and an observed visual brightness $V = 4^m.60$ we find: $A_V = 2^m.4$. The colour excess $E_{B-V} = 0^m.33$ gives: $A_V/E_{B-V} \approx 7$, which, as we will show in section 5, corresponds to $E_{V-K}/E_{B-V} \approx 6$.

Apart from the large values of E_{V-K}/E_{B-V} which have been marked in figure 3 a slow variation with galactic longitude seems to be present (dotted line). We are inclined to conclude also that A_V/E_{B-V} must exhibit a similar variation. The dotted line in figure 3 is the best smooth fit to the plotted points, omitting the large, marked, values. A minimum value seems to be reached at $l^{II} = 110°$. We note that nearly all stars used for the construction of the dotted line are near to the galactic equator, while some of the regions of large deviation (II Per and Orion) are at greater galactic latitude. It is further of interest that the four largest colour-excess ratios are found where E_{B-V} is smaller than $0^m.8$ and that the largest values occur in the Orion Nebula region where E_{B-V} is only $0^m.3$.

Next we wish to analyze the colour-excess ratio E_{V-J}/E_{B-V}. The values for HD 183143 and VI Cygni No. 12 are 2.36 and 2.17, resp., with a weighted mean value of 2.22, considerably less than A_V/E_{B-V}. Assuming for the latter ratio a value of 3.1 we conclude that at the effective wavelength of the J filter $\frac{1}{3}$ of the visual extinction is left. Figure 4 shows a plot of E_{V-J}/E_{B-V} against galactic longitude for the same stars as in figure 3. The two figures show the same features, but somewhat less pronounced in the case of figure 4.

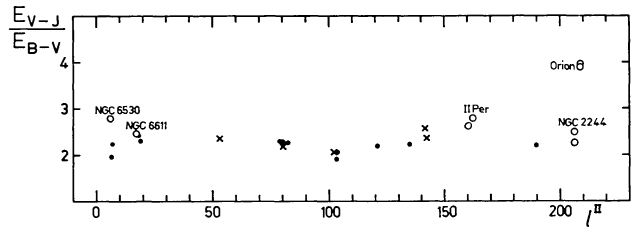

Fig. 4. E_{V-J}/E_{B-V} versus galactic longitude for all stars in table 2 with $E_{B-V} \geq 0^m.20$. Symbols have the same meaning as in figure 3.

Finally we will consider the colour-excess ratios

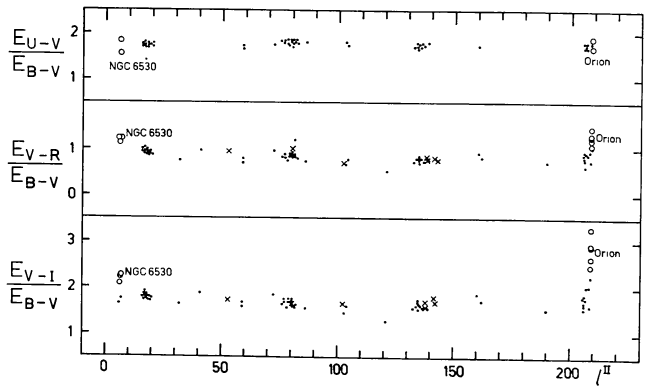

Fig. 5. E_{U-V}/E_{B-V}, E_{V-R}/E_{B-V} and E_{V-I}/E_{B-V} versus galactic longitude for all stars in table 2 with $E_{B-V} \geqslant 0^{m}.20$. The first colour-excess ratio has been plotted for the O stars only. Open circles refer to stars in NGC 6530 and the Orion Nebula, resp. Crosses represent late B-type supergiants.

E_{V-I}/E_{B-V}, E_{V-R}/E_{B-V} and E_{U-V}/E_{B-V}. Figure 5 shows these quantities plotted against galactic longitude, for all stars in table 2 with $E_{B-V} \geqslant 0^{m}.20$. E_{U-V}/E_{B-V} has been plotted only for O stars to prevent scatter due to the large range of intrinsic $U - V$ values among the early B stars. It is clear that the variation of E_{U-V}/E_{B-V} with galactic longitude is small. Two regions which have often received special attention are well represented in the diagram of figure 5; the average value of E_{U-V}/E_{B-V} in Cygnus (12 stars at $l^{II} \approx 80°$) is 1.83 ± 0.01 (m.e.) and in Perseus (10 stars at $l^{II} \approx 135°$) we find 1.75 ± 0.01 (m.e.). Recently WAMPLER (1961) has rediscussed the *UBV* material of HILTNER and JOHNSON (1956). From his data (table 1 of WAMPLER, 1961) we find for Cygnus and Perseus also 1.83 and 1.75, resp., if we interpolate for $(U - B)_0 = 1^{m}.15$, which is the adopted intrinsic colour of O stars in the present paper.

An inspection of figure 5 makes at once clear that relatively large values of E_{V-I}/E_{B-V} and E_{V-R}/E_{B-V} are reached in the Orion Nebula region. The deviations are smaller than in the previous diagrams (figures 3 and 4), which include light farther into the infrared. The general variation with wavelength of E_{V-I}/E_{B-V} and E_{V-R}/E_{B-V} is small; the only conclusion can be that the values in the region $70° < l^{II} < 150°$ are smaller than in the region $0° < l^{II} < 20°$, in agreement with the diagrams of figures 3 and 4. In the region $0° < l^{II} < 20°$ is also NGC 6530, whose stars seem to have large values of E_{V-I}/E_{B-V} and E_{V-R}/E_{B-V}, again in agreement with figures 3 and 4.

5. The ratio $R = A_V/E_{B-V}$.

Due to the circumstance that a considerable number of stars in table 2 have been observed in the far infrared where the interstellar extinction is small, a rather direct estimate can be made of R, the ratio of visual to selective extinction on the *BV* system. We have given already some considerations in this respect in the preceding section and have concluded that in the case of the filter K (2.1 μ) the interstellar extinction is probably only 8–14% of the visual extinction. The range corresponds to an adopted range of 3.0 to 3.2 for R, based on existing estimates of R from statistical studies in star clusters.

An independent way of deriving R is to extrapolate the observed relation between extinction and wavelength to infinite wavelength. Actually, the relation between wavelength and extinction is not observed directly. The extinction is derived from the observations by using assumed values of intrinsic colours. Also the wavelength is not an accurately known parameter as a consequence of the wide band filters. Some characteristics of the filters are given in table 1. λ_e has been computed, using the intensity distribution of a black body at 22000 °K. Temperatures of stars in this investigation may vary from 50000 °K to 10000 °K; however, the value of λ_e is almost independent of a corresponding variation of $I(\lambda)$ as long as we accept black-body radiation. The only irregularity of some importance is the Balmer jump, which affects λ_e of the filter U for late B stars. The functions $S(\lambda)$ used for the computation of λ_m and λ_e have been published by JOHNSON and MITCHELL (1962).

It has been shown that λ_e is the effective wavelength for extinction measurements in first-order approximation. The use of λ_m for this purpose would require small magnitude corrections, formulae for which are given in KING's (1952) article. The resulting accuracy is somewhat better than can be obtained with the direct use of λ_e, without magnitude corrections. However, the difference is small and we will continue to use the more convenient quantity. It is doubtful whether a precise reduction of the heterochromatic observations to monochromatic extinction values is worthwhile with the existing response data at hand.

We now proceed with the derivation of R from the "observed" relation between extinction and wave-

length. The extrapolation to infinite wavelength will be guided by using the theoretical extinction curves computed by VAN DE HULST (1949), some of which are known to be in good agreement with observational data. We will follow Van de Hulst's preference for his curve no. 15. This extinction curve will now first be compared with the observed extinction data of 4 O stars in Cygnus, which show colour excesses E_{B-V} larger than 1 magnitude. The extinctions A' are given in table 4a, normalized to $E_{B-V} = 1^m.00$ and $A'_V = 0^m.00$ consequently, $A'_B = 1^m.00$. The weighted mean values have been computed using weights E_{B-V}. The extinctions according to Van de Hulst's curve no. 15 have been calculated for the values of λ_e^{-1} in table 1, normalized to $A'_B = 1^m.00$ and $A'_K = -2^m.75$. This means that curve no. 15 will coincide with the observed curve for the values of λ_e^{-1} corresponding to the filters B and K (Our choice of these two points of coincidence is inspired by the consideration that the variation of detector sensitivity with wavelength is small in these two cases, which results in more accurate values of λ_e). As shown by the differences in the last line of table 4a the agreement is satisfactory, except for the R and U points. From narrow band photometry (DIVAN, 1956; BORGMAN, 1961) it is known that Van de Hulst's theoretical curves deviate in the ultraviolet from the observed data in the sense also found here. Figure 6 (curve "Cygnus") illustrates the conclusions to be drawn from table 4a. The R residual can be made zero by adopting for λ_e^{-1} the value 1.50 μ^{-1} instead

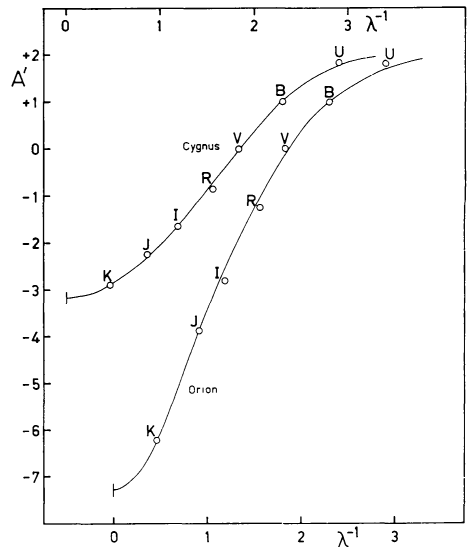

Fig. 6. Normalized extinction values versus λ^{-1}. Open circles are observations, the drawn curves are the theoretical extinction laws of Van de Hulst.

TABLE 4a

Extinction in the Cygnus region

Star	A'_∞	A'_L	A'_K	A'_J	A'_I	A'_R	A'_V	A'_B	A'_U
	m	m	m	m	m	m	m	m	m
HD 229196			− 2.90	− 2.29	− 1.69	− 0.85	0.00	1.00	1.79
VI Cygni 9			− 2.82	− 2.21	− 1.60	− 0.89	0.00	1.00	1.86
VI Cygni 10			− 2.92	− 2.28	− 1.70	− 0.88	0.00	1.00	1.85
HD 195592			− 2.94	− 2.25	− 1.63	− 0.79	0.00	1.00	1.78
Weighted mean			− 2.88	− 2.25	− 1.65	− 0.86	0.00	1.00	1.83
Curve no. 15	− 3.17	− 3.03	− 2.88	− 2.30	− 1.63	− 0.72	− 0.04	1.00	1.75
Difference			0.00	+ 0.05	− 0.02	− 0.14	+ 0.04	0.00	+ 0.08

TABLE 4b

Extinction in the region of the Orion Nebula

Star	A'_∞	A'_L	A'_K	A'_J	A'_I	A'_R	A'_V	A'_B	A'_U
	m	m	m	m	m	m	m	m	m
θ^1 Ori			− 6.31	− 3.88	− 2.91	− 1.21	0.00	1.00	1.76
θ^2 Ori			− 6.09	− 3.91	− 2.65	− 1.30	0.00	1.00	1.91
Weighted mean			− 6.22	− 3.89	− 2.81	− 1.25	0.00	1.00	1.82
Curve no. 3	− 7.29	− 6.70	− 6.22	− 3.85	− 2.53	− 1.02	− 0.09	1.00	1.70
Difference			0.00	− 0.04	− 0.28	− 0.23	+ 0.09	0.00	+ 0.12

of 1.56 μ^{-1} as has been assumed so far. Table 4a gives us: $A'_\infty = -3^m.17$, which means that the weighted mean value of R for the 4 Cygnus stars is 3.17. The corresponding colour-excess ratio $E_{V-K}/E_{B-V} = 2.88$; hence, R is equal to 1.10 times this colour-excess ratio. Thus, the extinction at the effective wavelength of the filter K is only 9% of the visual extinction.

The value of $A'_L = -3^m.03$ in table 4a has been read from the theoretical curve. It can be compared with the two determinations of E_{V-L}/E_{B-V} discussed in section 4 of this paper: 2.90 and 3.30 for VI Cygni no. 12 and HD 183143, resp., with a weighted mean value of 3.01. The agreement with the theoretical curve ($A'_L = -3^m.03$) is quite satisfactory, but should not be over-emphasized. HD 183143 is not a „Cygnus star", while VI Cygni no. 12 is extremely reddened, perhaps resulting in curved reddening lines. This is one of the reasons why we have left out the latter star from table 4a.

So far, we have considered only a small group of stars in Cygnus. From the analysis of the colour-excess ratios in section 4 these stars could be expected to exhibit an extinction curve which is representative of the majority of stars in table 2. We will now discuss the extreme case of the stars in the Orion Nebula. It is clear that here Van de Hulst's curve no. 15 is not a good model. In his paper, Van de Hulst has analyzed the extinction curve of θ^1 Ori observed by STEBBINS and WHITFORD (1945) for the spectral region 1 μ^{-1} to 3 μ^{-1}. He gives a number of alternative curves for θ^1 Ori and a good fit to our observations can be obtained with curve no. 3 of table 15 in Van de Hulst's paper. Table 4b gives the extinctions A' in the same fashion as table 4a, but for θ^1 Ori and θ^2 Ori. The fourth line gives the extinctions according to curve no. 3, cited above, normalized to $A'_B = 1^m.00$ and $A'_K = -6^m.22$. The differences in the last line are satisfactorily small, except possibly for the R and I points. These two residuals can be made zero by a change of the values of λ_e^{-1} to 1.50 μ^{-1} and 1.13 μ^{-1}, resp. When comparing the residuals in the last lines of tables 4a and 4b it should be remembered that the residuals for the Orion stars are expected to be larger because the normalized extinction curve shows more rapid variation of extinction with wavelength in the red and infrared; moreover, the observational data are based on stars of moderate reddening only. The data for the Orion Nebula stars in table 4b have been entered in figure 6.

Table 4b gives us directly the value of R for the two Orion Nebula stars; $R = 7.29$. The corresponding colour-excess ratio $E_{V-K}/E_{B-V} = 6.22$, so we find $R = 1.17\, E_{V-K}/E_{B-V}$. The factor for the Cygnus stars of table 4a is 1.10. It is fortunate that for these two extreme extinction curves the relation between R and E_{V-K}/E_{B-V} is not greatly different. No doubt this situation is due to the circumstance that the interstellar

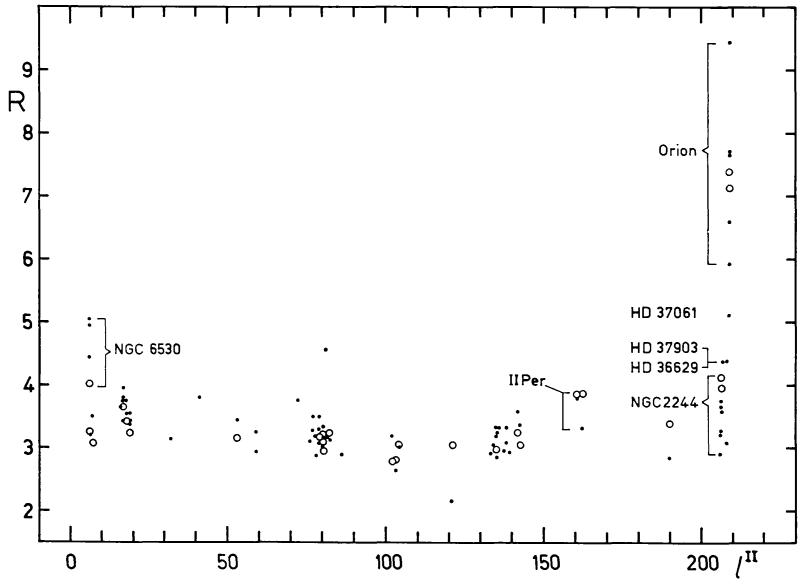

Fig. 7. $R = A_V/E_{B-V}$ versus galactic longitude for all stars in table 2 with $E_{B-V} \geq 0^m.20$. Dots indicate values computed from E_{V-I}/E_{B-V}. Open circles represent the values computed from E_{V-K}/E_{B-V}.

extinction at the effective wavelength of the filter K is so small, ranging from 9% (Cygnus) to 15% (Orion) of the visual extinction. If we put $R = f \times E_{V-K}/E_{B-V}$ and we assume that the small variation of f with E_{V-K}/E_{B-V} is real and can be interpolated by a linear relation, we find:

$$R = (1.04 + 0.021\ E_{V-K}/E_{B-V})\ E_{V-K}/E_{B-V}\ .$$

Our analysis so far shows that R can be predicted with reasonable accuracy from observed values of E_{V-K}/E_{B-V}. However, the latter quantity can be observed only for relatively bright stars. It may be of interest to investigate whether R can be predicted also from a more easily observed colour-excess ratio, such as E_{V-I}/E_{B-V}. If we write $R = g \times E_{V-I}/E_{B-V}$, then $g = 1.92$ for the stars of table 4a (Cygnus) and $g = 2.87$ for the stars in table 4b (Orion). The variation of g with E_{V-I}/E_{B-V} is quite pronounced; assuming a linear relation between g and E_{V-I}/E_{B-V} we find:

$$R = (0.96 + 0.58\ E_{V-I}/E_{B-V})\ E_{V-I}/E_{B-V}\ .$$

This interpolation formula, derived from the extreme values of R, may seem more risky than it is. With the exception of the Orion stars the colour-excess ratio E_{V-I}/E_{B-V} is always near to the value found for the Cygnus stars.

In figure 7 we have plotted the values of R as computed from E_{V-K}/E_{B-V} (open circles) and E_{V-I}/E_{B-V} (dots) against galactic longitude. The large scatter, even within a physical group is undoubtedly partly due to the circumstance that we have included all stars with $E_{B-V} > 0^m.20$. The smallest colour excesses of this material result in the least accurate colour-excess ratios and R values. This statement is quite evident, but can be checked by an inspection of figure 7: the range of R decreases in the order Orion – NGC 2244 – Cygnus (the clustering at $l^{II} \approx 80°$) while the average colour excess increases in the same order. There is one large value of R among the Cygnus stars: HD 188209 shows $R = 4.6$, but the colour excesses are small (e.g. $E_{B-V} = 0^m.21$). The minor scatter for the group of Cygnus stars suggests that the range of R for a small region in the sky can be small. Figure 7 seems to indicate that the scatter of the dots is somewhat larger compared to the open circles; however, the latter material is not large enough to conclude that the determination of R from E_{V-I}/E_{B-V} is inferior, though this conclusion can certainly be expected.

TABLE 5
Values of R

Group	n	R	m.e.	E_{B-V}
				m
NGC 6530	4	4.50	± 0.21	0.33
NGC 6611	7	3.71	0.03	0.84
VI Cygni	9	3.12	0.03	2.01
I Persei	15	3.16	0.04	0.75
II Persei	4	3.75	0.07	0.29
NGC 2244	7	3.65	0.14	0.47
Orion Neb.	7	7.37	0.25	0.30

Table 5 lists values of R determined from E_{V-K}/E_{B-V} and E_{V-I}/E_{B-V} by the formulae above. Double weight was given to the determinations from E_{V-K}/E_{B-V}. The number n is the total number of colour-excess ratios in the group. The mean error is simply the mean error as computed from the scatter of the individual values of R. It includes neither the uncertainties connected with the extrapolation procedure of the extinction curve nor the errors in the adopted values of the intrinsic colours. The extrapolation error might be in the order of 0.1 for $R \approx 3$ and 0.3 for $4 < R < 7$. In this connection we may mention the possibility that the curvature of the extinction curve in the far infrared is less pronounced than follows from Van de Hulst's models; we have a tentative indication of such deviating behaviour in observations of μ Cep, extending to 5 μ (not discussed in the present paper). The influence of errors in adopted intrinsic colours depends on the average colour excess in each group. The resulting uncertainty in the value of R may be negligible for the stars in VI Cygni and I Per (the group of stars around and including the Perseus double cluster) but may be considerable for the Orion stars, which show an unfortunate combination of small colour excesses and peculiar spectra. However, even in Orion the error of R should not be larger than 1. It is of interest to note that the values of R in Cygnus and Perseus (represented by VI Cygni and I Persei) are the same, in spite of the fact that distinct variations of the reddening law in the visible and ultraviolet light seem to exist (BORGMAN, 1961; WAMPLER, 1961; see also section 4 of the present paper). The tentative conclusion is that a prediction of R from the behaviour of the extinction curve in the visible and ultraviolet light is not possible. It also

follows that the situation is more complicated than suggested by the model curves of Van de Hulst.

6. Photometric distances

The large range of R (3.1 to 7.4) found in the preceding section indicates that a determination of the extinction term in the photometric distance formula should be based on more detailed knowledge of R than is usually available. Until now all distance determinations have been based on a constant value of $R \approx 3.1$. This procedure may result in overestimates of the distance modulus by the following amounts: NGC 6530, $0^m.5$; NGC 6611, $0^m.5$; II Persei, $0^m.2$; NGC 2244, $0^m.3$; Orion Nebula, $1^m.0$. These values have been computed from the values of R and the average E_{B-V} as given in table 5. It is of interest to note that the largest values of R tend to occur in young clusters, having small values of E_{B-V}; we are tempted to suggest that the interstellar material with the anomalous reddening law exists in or near these groups. This conclusion is quite evident in case of the Orion Nebula stars. In this connection it should be noted that HD 37061 and HD 37903, in order of increasing distances from the Orion Nebula show more normal values of R in the same order (see figure 7).

It is reassuring that the value of R for O and B stars is probably independent of the colour excess (BLANCO and LENNON, 1961).

Conclusion

The law of interstellar reddening shows variations which result in a considerable range of $R = A_V/E_{B-V}$ (3.1 in Cygnus to 7.4 in the Orion Nebula region). The value of R can be estimated from a colour-excess ratio, which should preferably include an observation in the 2 μ region. The colour-excess ratio E_{V-K}/E_{B-V} complies with this requirement; its numerical value comes close to R. A multiplication factor of 1.10 to 1.17 has been found, depending on the value of E_{V-K}/E_{B-V}. The accuracy of an individual determination of R depends on the accuracy of adopted intrinsic colours and the amount of the colour excesses.

We have suggested that the larger values of R arise in regions of young, hot stars; this makes it likely that the lower value of 3.1 is associated with the large portion of the interstellar material that exists without noticeable interaction with the hot stars.

This research, including the development of the infrared photometer apparatus, has been supported in part by the National Science Foundation.

References

A. BLAAUW, C. S. GUM, J. L. PAWSEY and G. WESTERHOUT, 1960, *M. N.* **121** 123
V. M. BLANCO and C. J. LENNON, 1961, *A.J.* **66** 524
J. BORGMAN, 1961, *B.A.N* **16** 99 (No. 512)
J. BORGMAN and H. L. JOHNSON. 1962, *Ap.J.* **135** 306
L. DIVAN, 1954, *Ann. d'Aph.* **17** 456
W. A. HILTNER, 1956, *Ap. J. Suppl. Series* **2** 389
W. A. HILTNER and H. L. JOHNSON, 1956, *Ap. J.* **124** 367
H. C. VAN DE HULST, 1949, *Rech. Astr. de l'Obs. d'Utrecht* **11** (part 2) 1
H. L. JOHNSON, 1951, *Ap. J.* **114** 522
H. L. JOHNSON, 1958, *Lowell Bulletin* **4** 37
H. L. JOHNSON 1962, *Ap. J.* **135** 69
H. L. JOHNSON, A. A. HOAG, B. IRIARTE, R. I. MITCHELL and K. L. HALLAM, 1961, *Lowell Bulletin* **5** 133
H. L. JOHNSON and B. IRIARTE, 1958, *Lowell Bulletin* **4** 47
H. L. JOHNSON and R. I. MITCHELL, 1962, *Contr. Lunar and Plan. Lab.*, No. 14
H. L. JOHNSON and W. W. MORGAN, 1953, *Ap.* J. **117** 313
H. L. JOHNSON and W. W. MORGAN, 1955, *Ap. J.* **122** 429
I. KING, 1952, *A. J.* **57** 253
S. SHARPLESS, 1952, *Ap. J.* **116** 251
S. SHARPLESS, 1957, *P. A. S. P.* **69** 239
J. STEBBINS and A. E. WHITFORD, 1945, *Ap. J.* **102** 339
E. J. WAMPLER, 1961, *Ap. J.* **134** 861
A. E. WHITFORD, 1958, *A. J.* **63** 201